Characterization of ageing of solid electrolyte sensors by impedance spectroscopy

J. Zosel[1], A. Solbach[2], D. Tuchtenhagen[2], C. Treu[3], H. Heelemann[3], F. Gerlach[1],
K. Ahlborn[1], U. Guth[1],
[1]Meinsberg Kurt-Schwabe Research Institute, Kurt-Schwabe-Straße 4,
D-04720 Ziegra-Knobelsdorf, Germany
[2]ACEOS GmbH, Karolinenstraße 108, D-90763 Fürth, Germany
[3]Software & Technologie Glas GmbH, Kiekebuscher Weg 14, D-03050 Cottbus, Germany

1 Outline of the problem

Ageing processes are the most important limitations for long-term stability and service life of electrochemical sensors. Side conditions of application [1], sensor operation [2], the sensor construction [3] as well as the sensor materials [4] determine the nature and velocity of these processes. Solid electrolyte sensors operating at temperatures above 500 °C show some characteristic ageing phenomena like:

- electrolyte degradation by crack formation and/or reaction with electrode materials or alkali dust,
- electrode delamination from the electrolyte or morphological changes of the electrode materials,
- diffusion of inhibiting chemical species like sulphur or dust particles to the electrochemical active sites,
- changes of diffusion barriers of amperometric sensors and
- changes at the heating devices by material degradation or degradation of the cover layer.

Very often the overall ageing process is driven by an interaction of these phenomena. This complicates their clarification and therefore the proper assortment of counteractive measures. In this paper electrochemical impedance spectroscopy (EIS) was combined with different X-ray-techniques to investigate ageing processes at two different kinds of solid electrolyte high temperature sensors. One kind concerns potentiometric Nernst type sensors for the measurement of equilibrium oxygen concentration in the exhaust of glass melts that are operated at temperatures between 1000 and 1500 °C [5]. The second type concerns amperometric oxygen sensors manufactured completely with thick film technology and applied for breath gas monitoring [6].

2 Innovation of solution

The application of potentiometric oxygen sensors for combustion control of glass melting processes is connected with large temperature gradients, condensation of melt components at the sensor surface and temporally occurring reducing conditions in the exhaust gas. These side conditions are responsible for some serious ageing processes, which were investigated by EIS combined with X-ray photoelectron spectroscopy (XPS) and scanning electron microscopy (SEM). Amperometric solid electrolyte sensors [7] are equipped with diffusion barriers triggering sometimes slowly drifting diffusivity due to changes of the pores. This process can be accompanied by agglomeration of inhibiting substances at the triple phase boundary. Optimized equivalent circuits were used for interpretation of impedance spectra to distinguish between these ageing processes.

3 Technical realisation

3.1 Nernst-type potentiometric oxygen sensor

Potentiometric sensors for oxygen measurement in exhaust of glass melting processes are not self-heated but operated at the ambient temperature of the measuring atmosphere ranging between 1000 and 1500 °C. As shown in Fig. 1 schematically, the one-side closed solid electrolyte tube is made of yttria stabilized zirconia (YSZ) and cemented into an alumina tube. The inner side of the YSZ tube a ceramic capillary provides the reference potential by air rinsed inner electrode. The supporting alumina tube contains a thermocouple for the temperature measurement and the connecting wires for the electrodes. To ensure sensor positioning in the appropriate measurement position of the regenerator, the alumina tube length ranges around 1 m. For the majority of application sites the sensor is also equipped with an outer protecting tube with front-side opening for measuring gas entrance.

To characterize the actual sensor state at the laboratory the outer electrode potential is measured in air by rinsing the inner electrode with a gas mixture of 3 Vol.-% H_2 and 3 Vol.-% H_2O in N_2. Passing this test with the expected potential of 938 mV at 800 °C, given by the equation published in [8], the sensor is investigated than by impedance spectroscopy at temperatures between 1000 and 1400 °C in different gas mixtures. Sensors with pronounced states of damage after usage are investigated by SEM as well as XPS to correlate the results of impedance measurements with changes at microscopic scale.

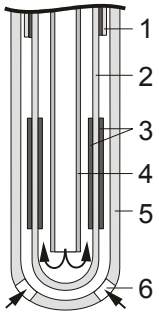

Fig. 1:
Schematic drawing of the potentiometric sensor for glass melting process
1 supporting tube (alumina) with thermo couple
2 zirconia solid electrolyte
3 platinum electrodes
4 reference air supply
5 alumina protecting tube
6 gas inlet

3.2 Planar amperometric oxygen sensor

Amperometric sensors, given in Fig. 2, of different states of ageing were investigated at various temperatures, oxygen partial pressures and polarization potentials by means of EIS. These sensors are equipped with a heater on the reverse side, made of screen printed Pt conduction paths. Temperature control of the sensor is performed by an additional voltage measurement at the two hot ends of the heater at the sensor tip, providing a highly sensitive power measurement. Pyrometric measurements with a spatial resolution of 0.3 mm of the electrode surface were performed to correlate the applied heating power with the absolute surface temperature. Sensors with different designs were characterised with electrochemical current/potential as well as impedance measurements in O_2/N_2 gas mixtures with oxygen partial pressure between 0.5 ... 200 kPa at temperatures between 500 ... 615 °C. Equivalent circuits were developed for the elements of the electrochemical cells and adapted to the experimental results. Similar to the procedure performed at the potentiometric sensors additional investigations were carried out with SEM.

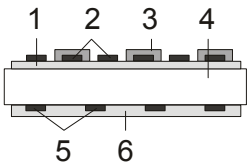

Fig. 2:
Schematic drawing of the amperometric sensor
1 zirconia solid electrolyte
2 platinum electrodes
3 diffusion barrier
4 alumina substrate
5 heater
6 cover

4 Results

4.1 Nernst-type potentiometric oxygen sensor

The curves in Fig. 3 show impedance plots of a newly fabricated potentiometric oxygen sensor in comparison to a sensor operated more than five years in combustion gases over a glass melt, which is still working. The plots enable to distinguish between electrolyte and polarization resistances and therefore to characterize ageing processes. While the new sensor provide a DC resistance below 12 Ω, the aged one exhibit values between 4 ... 5 kΩ when operated in air. The curves of the aged sensor exhibit an enlarged bow of the outer electrode, indicating a large decrease of contact area between the Pt-electrode and the solid electrolyte.

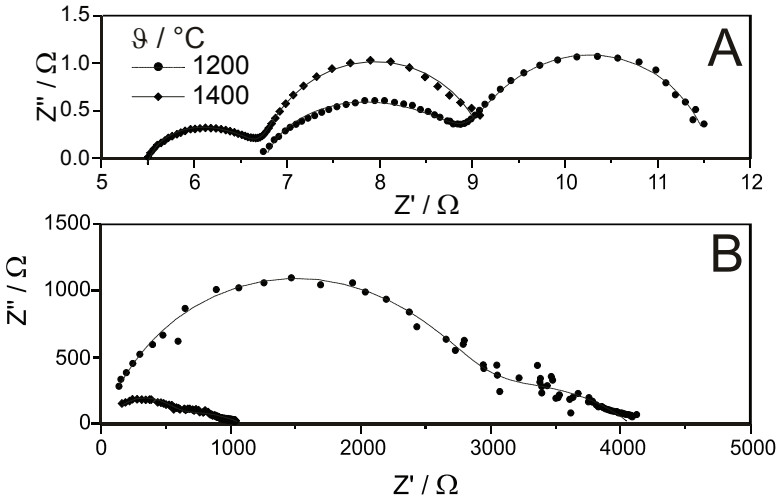

Fig. 3:
Nyquist plots of the impedance of two potentiometric oxygen sensors for combustion control in glass melts, A new sensor, B sensor with more than five years in a glass melt, still working

The sensors, illustrated in Fig. 4 as examples for the great variety of possible ageing phenomena, were attacked by corrosion by condensed glass material to the alumina tube (A), and by degradation of the YSZ tube due to different corrosion effects and thermal shock resulting in cracks (B). Another ageing phenomenon, visible in Fig. 4 B, is the loss of Platinum from the outer electrode due to evaporation.

Fig. 4:
Examples for different possible damage states:
A) sensor from a glass melt with soda-lime glass
B) degradation of the solid electrolyte by corrosion and thermal shock

Pt and Rh evaporated from the electrode sometimes condense at colder regions of the supporting alumina tube, which could be shown by XPS and SEM investigations. The results in Fig. 5 describe an example of condensed Pt/Rh crystals. The two extracts of the corresponding XPS spectrum indicate that both elements are found in the condensate. The Pt 4f5/2-peak is dominated by the Al 2p-peak but the Pt 4f7/2 peak can be correlated with the presence of Pt. The Rh 3d5/2-Peak dominates the curve in the right part of the spectrum in Fig. 5. The coexistent Rh 3d3/2-Peak is translated by 4.74 eV to higher binding energy and therefore only half visible. The spectrum indicates also two oxidation states of Rh.

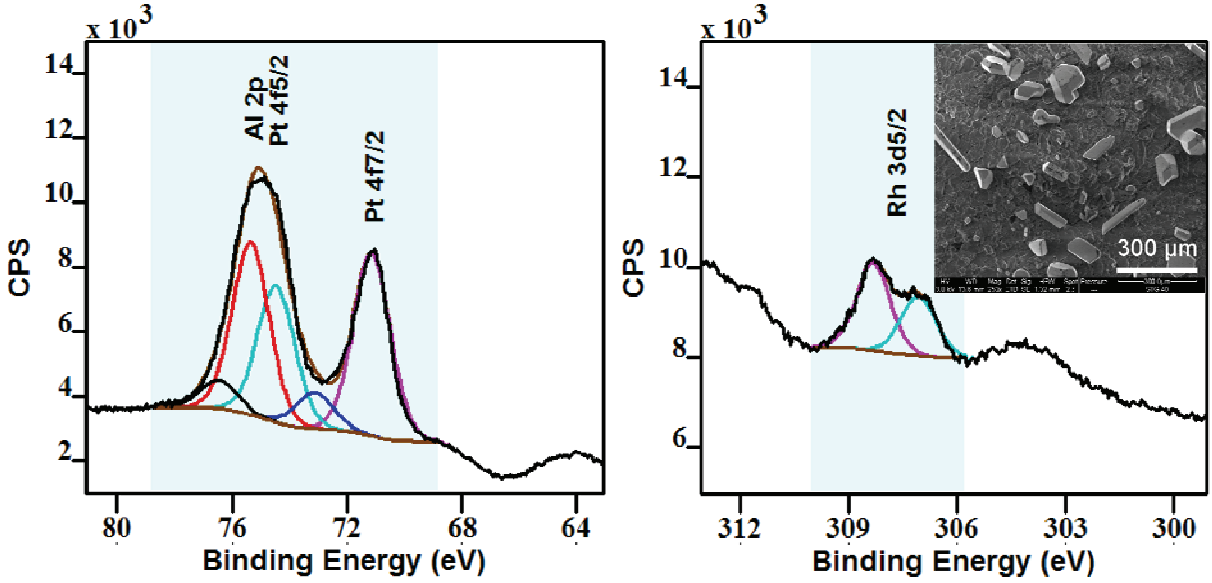

Fig. 5: XPS spectrum and SEM picture of condensed Pt/Rh particles

4.2 Planar amperometric oxygen sensor

The SEM picture of the breaking edge of a planar amperometric oxygen sensor according to Fig. 6 illustrates the dimensions of the different functional layers.

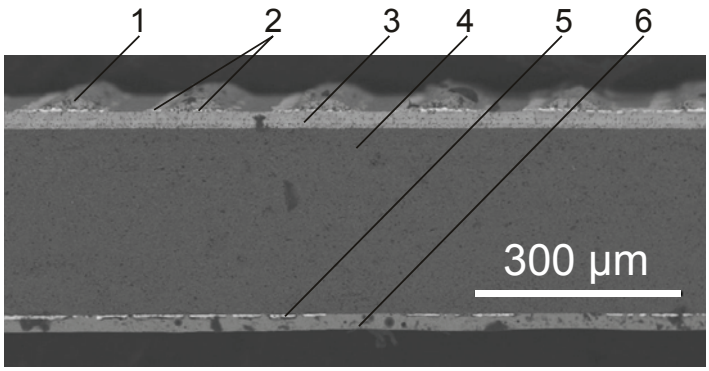

Fig. 6:
SEM picture of the breaking edge of a planar amperometric oxygen sensor:
1: diffusion barrier
2: Pt electrodes
3: YSZ solid electrolyte
4: alumina substrate
5: heater
6: cover

The SEM-investigations, which are absolutely necessary for the optimization of thick film technology, indicated only sporadically structural changes at sensor structures due to ageing processes. One of the investigated samples shows a contrast change at the electrode surface, caused by a longer measurement in a catalyst damaging environment. This contrast change could be correlated by electrochemical measurements with pronounced electrode passivation.

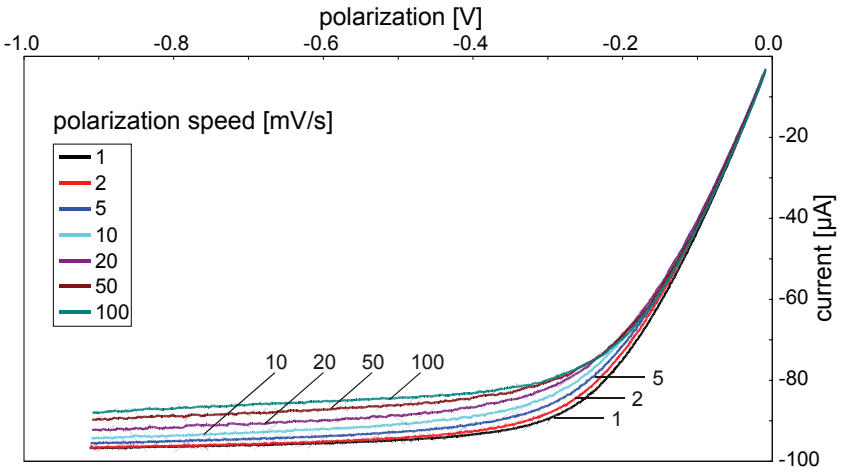

Fig. 7:

CV-measurements at an amperometric solid electrolyte sensor according to Fig. 2 in air,

sensor temperature 600 °C

As shown in Fig. 7, CV-measurements were performed at a medium aged planar sensor according to Fig. 2. The results exhibit pronounced plateaus of diffusion limiting current at polarization voltage between -400 ... -900 mV. The differences between the curves with different polarization speed are probably caused by delayed pore diffusion.

An example for impedance metric behaviour of planar oxygen sensors in air is shown in Fig. 8. The curves taken at different temperatures illustrate the expected decreasing sensor resistance with increasing temperature. The phase courses indicate different capacitive elements in the equivalent circuit. One of them acting in the high frequency region could be connected to the solid electrolyte. This element is only visible in the Bode plot, which is chosen here in contrast to Fig. 3. It could be shown that a model with four elements, containing a parallel circuit of a resistance and a constant phase element (CPE) can be fitted to the results with maximum error < 100 mΩ for both real and imaginary part of the spectrum. Some parts of the equivalent circuit were designed according to results published elsewhere:

- for the solid electrolyte [9]
- for the triple phase boundary [10]

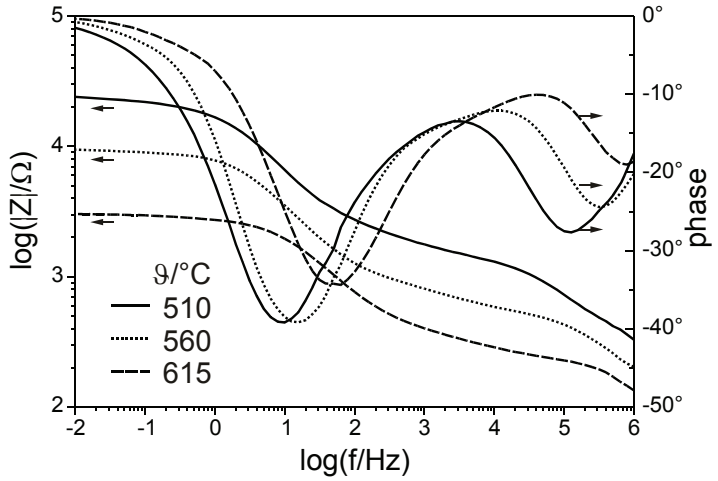

Fig. 8:
Bode plots of impedance of an amperometric solid electrolyte sensor at different temperatures in synthetic air,
cathode potential 0 mV

The model was validated by measurements at different sensors, temperatures and gas compositions. It allows extracting the values for electrolyte and polarization resistances. An example for the temperature dependence of cathode polarization and electrolyte resistance is shown in Fig. 9. The Arrhenius plots indicate activation energies between 70 ... 120 kJ/mol for both parameters.

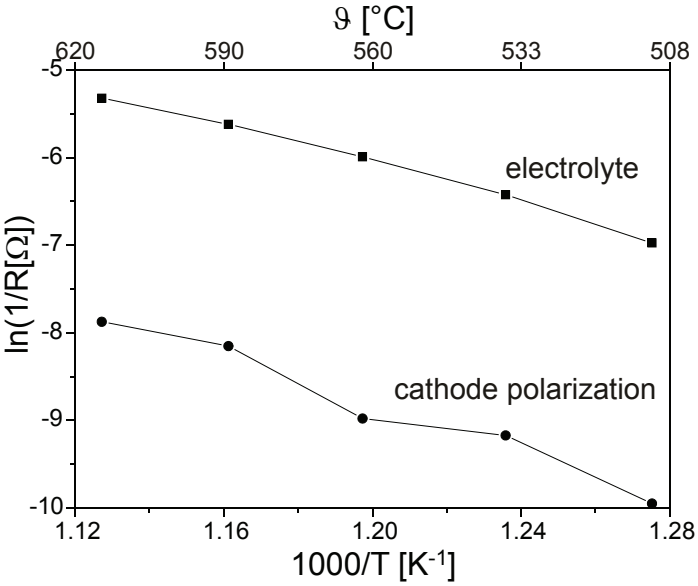

Fig. 9:
Arrhenius plots of the electrolyte and cathode polarization resistances extracted from curves in Fig. 8

Conclusions

A strategy for investigation of ageing processes including impedance spectroscopy and different X-ray diagnostics was successfully adapted to two different kinds of solid electrolyte high temperature sensors. The results enable not only to distinguish between different ageing phenomena but also to assort appropriate counteractive measures. Potentiometric sensors for oxygen measurement in exhaust gas of glass melting processes are exposed to a great variety of ageing phenomena like corrosion, electrode evaporation, electrode blocking by condensed glass layer and material degradation. Some of these phenomena can be clarified by electrochemical measurements and correlation of these results with XPS and SEM investigations.

Planar amperometric solid electrolyte sensors manufactured completely by thick film technique and applied for breath gas monitoring show ageing processes, which are triggered mainly by their design and materials. These processes concern the change of the diffusion barrier and the interaction between the electrodes and the diffusion barrier. Sometimes also cracks in the solid electrolyte can occur.

The functional elements can be modelled by an equivalent circuit containing four elements with a resistance and a constant phase element in parallel. Application of the model enables the separation of the individual changes of every functional element.

Literature

[1] F. Rettig, R. Moos, C. Plog, Sensors and Actuators B 93(2003) 36-42.
[2] M. Bode, P. Hauptmann, H. Rau, Sensors and Actuators B 7 (1992) 733-737.
[3] W. Oelßner, J. Zosel, U. Guth, T. Pechstein, W. Babel, J. G. Connery, C. Demuth, M. Grote Gansey, J. B. Verburg, Sensors and Actuators B 105, (2005) 104-117.
[4] K. Obata, S. Matsushima, Sensors and Actuators B 139 (2009) 435-439.
[5] H. Heelemann, Silikattechnik 38 (1987) Issue 7, 224-227.
[6] D. Tuchtenhagen, G. Jung, Patent WO 2006/005332 A3 (2006).
[7] C. Lopez-Gandara et al., Sensors and Actuators B 140 (2009) 432–438.
[8] H.-H. Möbius, in: Sensors, Vol. 3 (W. Göpel, J. Hesse, J. N. Zemel), VCH, Weinheim, 1991, p. 1114.
[9] J. v. Herle, A. J. McEvoy, K. Ravindranathan Thampi, J. Mat. Sci. 29 (1994) 3691-3701.
[10] A. K. Opitz, J. Fleig, Solid State Ionics 181 (2010) 684-693.

Acknowledgement
The support of the Federal Ministry of Economics and Technology (support codes KF0137601DA5 and KF2218303AB9) is gratefully acknowledged.